Combined Refinement of Diffusion Coefficients Applied on the Nb-C and Nb-N Systems

DAVID RAFAJA, WALTER LENGAUER, HERBERT WIESENBERGER, and MANECH JOGUET

A novel technique was used for the calculation of diffusion coefficients in the niobium carbides and nitrides prepared by reaction diffusion. The temperature ranges investigated were 1500 °C to 2100 °C for the Nb-C system and 1400 °C to 1800 °C for the Nb-N system. Three independent theoretical approaches were applied and their results are compared. In the metalloid-rich phases, the concentration-dependent diffusion coefficients were calculated from the concentration profiles; two models of layer growth were used to obtain the concentration-independent diffusion coefficients in all phases. It was found that the diffusion coefficient of carbon in δ-NbC_{1-x} shows a decrease with increasing metalloid concentration, whereas the diffusivity of nitrogen in δ-NbN_{1-x} is nearly independent of the nonmetal concentration. The concentration dependence of the carbon diffusion coefficients in δ-NbC_{1-x} is a result of a lower activation energy of carbon diffusion in the substoichiometric δ-NbC_{1-x} than in the δ-NbC. On the contrary, the activation energy of nitrogen in δ-NbN_{1-x} does not change with the nitrogen concentration. This behavior could be explained by the different occupancies of metal sublattices, which remain constant in δ-NbC_{1-x} but decrease with increasing nonmetal concentration in δ-NbN_{1-x}.

I. INTRODUCTION

DIFFUSION is an important phenomenon, especially in materials considered for high-temperature applications where it occurs in both production and use. To evaluate diffusivities, to model the concentration profiles arising during the diffusion process, and to simulate the phase band evolution in the Nb-C and Nb-N systems, three approaches were used: (1) an analytical solution of diffusion equations for the concentration profile (Section II–B), (2) an analytical solution of diffusion equations for the phase boundary movement (Section II–C–1), and (3) a numerical solution of diffusion equations that yielded both the development of the phase band structure and the concentration profiles in all phases (Section II–C–2).

Diffusion coefficients are usually calculated from the first derivative of the measured concentration profile. This technique is applied predominantly to solid/solid diffusion couples (*e.g.*, References 1 and 2), but it can be modified to be used for gas/solid diffusion. Unfortunately, as this method works with derivatives, it is very sensitive to the scatter in the measured concentrations. Thus, it is not practicable for calculating the diffusivities of light elements. Therefore, as in the first technique (Section II–B), the approximation of the measured concentration profile by a function, which is the analytical solution of the diffusion equations for concentration profiles, was applied by taking into account that the diffusion coefficient may depend on the concentration of the in-diffusing species. This method can only be employed for the calculation of diffusion coefficients in the metalloid-rich phases of Nb-C and Nb-N, as the concentration profiles in the intermediate phases Nb_2C and Nb_2N are very flat[3,4] and the maximum concentrations of carbon and nitrogen in the respective solid solution are low.

Diffusion coefficients in the intermediate phases can be obtained from layer growth. For the reaction diffusion, several models of layer growth were reported in the literature. However, not all of them offer a suitable tool for the evaluation of diffusion coefficients. As already stated by Jost,[5] the complete set of diffusion coefficients cannot be obtained from only the layer growth investigated in a series of diffusion experiments, which were carried out with samples having an infinite geometry. An exception is when one diffusion coefficient is known. On the other hand, diffusion coefficients in all phases can be calculated exclusively from layer growth if the finite sample geometry is involved, which we have shown recently.[6] This technique was used here as the second method (Section II–C–1). A similar approach, which is also based on the analytical solution of the diffusion equation, was described by Somers and Mittemeijer.[7]

For the third approach (Section II–C–2), the forward finite differences (FFD) method was applied, similar to that suggested by Pawel.[8] This method has great flexibility in the starting conditions and in the advance of the diffusion process.[9] Furthermore, the FFD method works consecutively. Thus, it is capable of simulating the morphological results of reactive diffusion in finite systems, where the layer growth, the development of individual concentration profiles, and the successive disappearance of phases in the core occurs.

DAVID RAFAJA, on leave from the Faculty of Mathematics and Physics, Charles University, CZ-121 16 Prague, Czech Republic, is Research Scientist, Institute for Chemical Technology of Inorganic Materials, Vienna University of Technology, A-1060 Vienna, Austria. WALTER LENGAUER, Professor, and HERBERT WIESENBERGER, Research Fellow, are with the Institute for Chemical Technology of Inorganic Materials, Vienna University of Technology. MANECH JOGUET, Graduate Student, is with the Laboratory of Metallurgy and Physical Chemistry of Materials, F-35043 Rennes, France.

Manuscript submitted July 9, 1997.

II. ONE-DIMENSIONAL DIFFUSION IN Nb-C AND Nb-N

A. *General*

In particular cases, the diffusivity of the nonmetal attending the diffusion process is substantially higher than the diffusivity of the host metal. This holds for the Nb-C system[10] as well as for the Nb-N system.[11] Consequently, the reactive diffusion in Nb-C and Nb-N can be regarded as a diffusion of carbon or nitrogen in a rigid metal grid, which is described by the one-dimensional second Fick's law.

$$\frac{\partial c}{\partial t} = \frac{\partial}{\partial x}\left(D\,\frac{\partial c}{\partial x}\right) \qquad [1]$$

where c is the concentration of in-diffusing species, D is the diffusion coefficient of the metalloid, x is the diffusion distance, and t is the diffusion time. In the analytical solution of diffusion equations, the diffusion time and the diffusion path are usually coupled by the Boltzmann–Matano variable, $y = x/(2\sqrt{t})$. This approach allows the partial differential Eq. [1] to be transformed into the ordinary differential Eq. [2], which can be solved analytically as

$$-2y\,\frac{dc}{dy} = \frac{d}{dy}\left(D\,\frac{dc}{dy}\right) \qquad [2]$$

The analytical solution of Eq. [2] has the following form (*e.g.*, Reference 12):

$$c(y) = \left(c^- - c^+\right) \frac{\displaystyle\int_{y(0)}^{y} \frac{1}{D(y')} \exp\left(-\int_{y(0)}^{y'} \frac{2y''\,dy''}{D(y'')}\right) dy'}{\displaystyle\int_{y(0)}^{y(\xi)} \frac{1}{D(y')} \exp\left(-\int_{y(0)}^{y'} \frac{2y''\,dy''}{D(y'')}\right) dy'} + c^+ \qquad [3]$$

where $y(0)$ and $y(\xi)$ are positions of the nonmetal-rich and the nonmetal-poor phase boundaries. The terms c^+ and c^- are the maximum and the minimum concentrations in the respective phase, which follow from the boundary conditions.

Frequently, the diffusion coefficients are assumed to be constant within individual phases. For many approaches, this is even a necessary assumption, because the respective calculus cannot handle the concentration dependence of diffusivity. Conversely, in the analytical formalism (Eq. [3]) the diffusion coefficient may be a function of the distance measured from the sample surface. Since the concentration of in-diffusing species is also a function of the distance, the diffusion coefficient is a function of concentration. The concentration dependence of diffusivity in binary systems has already been established to take an exponential form (*e.g.*, Reference 13).

$$D(c) = D_0 \exp\left[-a\left(c_{\max} - c\right)\right] \qquad [4]$$

B. *Concentration Profile Fitting*

The diffusion coefficient D_0 and its concentration dependence, which is characterized by the parameter a in Eq. [4], were refined by fitting the function in Eq. [3] to the measured concentration profiles. Taking the concentration dependence of the diffusion coefficient into account, the calculation of the concentration profile must be performed iteratively. In the first step, a starting concentration profile was estimated according to Eq. [3], where the diffusion coefficient was equal to D_0 (Eq. [4]) and was independent of the concentration. In the next step, the concentration dependence of the diffusion coefficient (the dependence of the diffusion coefficient on the distance from the sample surface) was adjusted by using Eq. [4]. The calculation of the concentration profile was then continued with the diffusion coefficient that depends on concentration. As Eq. [3] is a transcendent equation, the calculation of the concentration profile and the recalculation of the diffusion coefficient must be repeated until the differences between the subsequently calculated concentration profiles fall below a desirable limit. For refinement of the parameters D_0 and a, a least-squares method was used that searches for a global minimum upon a surface, which was composed from squared differences between the measured and the calculated concentrations calculated for a matrix of different D_0 and a values.

C. *Phase Boundary Movement*

1. *Analytical solution*

For the evaluation of the diffusion coefficients from the layer growth, the model published in Reference 6 was applied. This procedure is based on the investigation of layer growth in finite one-dimensional diffusion couples, in which a departure from the parabolic growth rate leading to a layer growth enhancement can be observed. In such a case, the finite sample geometry provides an additional parameter, *i.e.*, the sample thickness, which is necessary for the calculation of all diffusion coefficients.[5] The rate ''constant,'' which is independent of diffusion time in infinite samples, is then a function of the diffusion time and the sample thickness. Thus, a series of samples with different thicknesses or a series subjected to different diffusion times can be used. From the experimental point of view, the first choice is more appropriate than the latter. At best, small-angle wedge-shaped diffusion couples that fulfill the precondition of one-dimensional geometry[14] can be used.

2. *Numerical solution*

In the FFD method, each part of the concentration profile consisting of three adjacent points is approximated by a parabolic function, whereas the temporal evolution of the concentration profile is described linearly. This follows from the parabolic form of the diffusion Eq. [1]. Accordingly, the concentration profile is described by

$$c_i^{k+1} = \beta c_{i-1}^k + \left(1 - 2\beta\right) c_i^k + \beta c_{i+1}^k; \quad i = 2, \ldots, n-1 \qquad [5]$$

where the upper index labels the steps in the diffusion time and the lower index the steps in the diffusion direction. The coefficient β provides a coupling between the diffusion time and the diffusion distance, analogous to the Boltzmann–Matano variable y in the analytical solution. Unlike the Boltzmann–Matano variable, the diffusion coefficient D is included in β.

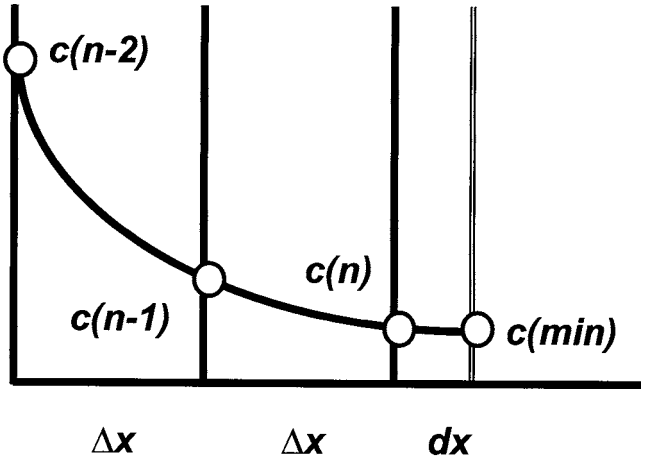

Fig. 1—Three-point parabolic approximation of concentration profiles among $c(n-2)$, $c(n-1)$, and $c(\min)$ was used for calculation of layer growth in the FFD method. The concentration at the last regular point of the grid, $c(n)$, was taken from the quadratic interpolation.

$$\beta = \frac{D\tau}{(\Delta x)^2} \qquad [6]$$

The diffusion time and the diffusion distance appear in Eq. [6] in the form of a temporal and a spatial step, τ and Δx. The value of β was set to 1/6, which satisfies the von Neumann stability criterion, $\beta \leq 1/2$ (*e.g.*, Reference 15).

As it follows from Eq. [5], only the concentrations inside individual phases can be calculated using FFD. The concentrations at the phase boundaries follow the boundary conditions, *i.e.*, they are equal to the maximum and the minimum concentrations allowed, for the respective phase, by the phase diagram. The starting nonmetal concentrations were set, according to the experimental conditions, to be equal to the maximum outside and zero inside the sample. As this model was designed for simulation of reaction diffusion in multiphase systems, the phases were assumed to appear simultaneously, similar to the well-known model of parabolic layer growth. Consequently, a more complex phase boundary structure must be established after the first temporal step τ that follows for a given spatial step Δx from Eq. [6]. The FFD method must be modified to be able to set up true starting concentration profiles and to also calculate correct phase boundary positions for short diffusion times.

The calculation of the starting phase boundary positions was carried out iteratively to balance the diffusion flows (J) at all phase boundaries, according to the one-dimensional continuity equation.

$$\frac{\partial c}{\partial t} = -\frac{\partial J}{\partial x} \qquad [7]$$

Initially, a steplike profile consisting of the phase boundary concentrations taken from the phase diagram was established. In all phases, the concentrations at the metalloid-rich phase boundaries were set to the maximum concentration, the concentrations in other points to the minimum one. From this distribution, the iterative routine yielded concentration profiles in all phases except the core (so to say, in the ''outer phases'') for an arbitrary diffusion time and for an arbitrary spatial step. The thickness of the individual layers was adjusted to attain an equilibrium between the diffusion flows at the phase boundaries. Finally, the real spatial and temporal steps were assigned in the individual phases. Considering the great differences among diffusion coefficients in the different phases, the partial diffusion times are substantially shorter in the outer phases than in the core. Therefore, in the outer phases, the procedure must be repeated until each sum of partial diffusion times is identical and equal to τ (the overall temporal step).

After the starting phase boundary structure and the initial concentration profiles within all phases have been established, the growth (dx) of individual layers was calculated from Eq. [8] using the ''regula falsi'' method.

$$J = -D\left(2\,\frac{c_{n-2}\,(\Delta x + dx) - c_{n-1}\,(2\,\Delta x + dx) + c_{\min}\,\Delta x}{2(\Delta x)^2 + \Delta x dx} + \frac{c_{n-1} - c_{n-2}}{\Delta x} + \frac{c_{n-2}\,(\Delta x + dx) - c_{n-1}\,(2\Delta x + dx) + c_{\min}\,\Delta x}{\Delta x\,(\Delta x + dx) + (\Delta x + dx)^2}\right) \qquad [8]$$

In Eq. [8], Δx is the regular step size in the grid, dx is the phase boundary displacement, c_{n-2} and c_{n-1} are concentrations in two regular points just before the nonmetal-poor phase boundary, $c_{\min}$ is the concentration at the nonmetal-poor phase boundary according to the phase diagram, D is the diffusion coefficient of the nonmetal in the phase being investigated, and J is the diffusion flow at the nonmetal-poor phase boundary. The concentration in the last regular point of the mesh (c_n) must be obtained from parabolic interpolation among points of the irregular grid (Figure 1).

The calculation was performed from the core toward the sample surface. The diffusion flow at the metalloid-rich phase boundary follows from the first derivative of the concentration profile; the diffusion flow at the metalloid-poor phase boundary of the next outer phase must be the same to attain the equilibrium in diffusion flows (Eq. [7]). Equa-

Table I. Summary of Homogeneity Ranges in the Nb-C System between 1500 °C and 2100 °C Used for the Calculation of Layer Growth*

	δ-NbC_{1-x}		β-Nb_2C		α-Nb(C)	
T (°C)	c (max) (mol/cm³)	c (min) (mol/cm³)	c (max) (mol/cm³)	c (min) (mol/cm³)	c (max) (mol/cm³)	c (min) (mol/cm³)
1503	0.0725	0.0564	0.0458	0.0419	0.0002	0
1700	0.0725	0.0557	0.0458	0.0419	0.0010	0
1896	0.0725	0.0545	0.0458	0.0419	0.0018	0
2093	0.0725	0.0544	0.0458	0.0419	0.0026	0

*The maximum concentration in δ-NbC_{1-x} corresponds to [C]/[Nb] = 1.

Table II. Summary of Homogeneity Ranges in the Nb-N System between 1400 °C and 1800 °C Used for the Calculation of Layer Growth*

	δ-NbN_{1-x}		β-Nb_2N		α-Nb(N)		
T (°C)	c (max) (mol/cm³)	c (min) (mol/cm³)	c (max) (mol/cm³)	c (min) (mol/cm³)	c (max) (mol/cm³)	c (min) (mol/cm³)	Applied N_2 Pressure (bar)
1400	0.0780	0.0550	0.0440	0.0370	0.0016	0	29.9 ± 0.2
1500	0.0710	0.0540	0.0435	0.0365	0.0020	0	4.1 ± 0.1
1600	0.0710	0.0525	0.0435	0.0365	0.0030	0	7.6 ± 0.1
1700	0.0710	0.0520	0.0420	0.0360	0.0038	0	14.3 ± 0.4
1800	0.0710	0.0500	0.0420	0.0340	0.0055	0	30.1 ± 0.2

*The surface concentration between 1500 °C and 1800 °C was kept constant and equal to [N]/[Nb] = 0.91. At 1400 °C, the surface concentration was [N]/[Nb] = 1.

Table III. Diffusion Coefficients of Carbon in Niobium and Niobium Carbides*

	D from the Profile Fitting			D from the Layer Growth (FFD)		
T (°C)	δ-NbC_{max} (cm²/s)	δ-NbC_{min} (cm²/s)	a (cm³/mol)	δ-NbC_{1-x} (cm²/s)	β-Nb_2C (cm²/s)	α-Nb(C) (cm²/s)
1503	$4.3(2) \times 10^{-12}$	$3.9(1) \times 10^{-11}$	137	$1.3(1) \times 10^{-11}$	$1.7(1) \times 10^{-11}$	$1.0(1) \times 10^{-10}$
1702	$6.7(5) \times 10^{-11}$	$3.5(4) \times 10^{-10}$	99	$1.9(1) \times 10^{-10}$	$2.7(3) \times 10^{-10}$	$1.0(1) \times 10^{-9}$
1896	$3.8(4) \times 10^{-10}$	$2.1(3) \times 10^{-9}$	94	$1.2(2) \times 10^{-9}$	$1.7(2) \times 10^{-9}$	$6.0(3) \times 10^{-9}$
2093	$2.5(1) \times 10^{-9}$	$9.1(4) \times 10^{-9}$	70	$9.3(4) \times 10^{-9}$	$1.2(1) \times 10^{-8}$	$2.5(1) \times 10^{-8}$

*The diffusion coefficients listed in the column labeled δ-NbC_{max} correspond to the maximum carbon concentration, and the diffusion coefficients listed in the column labeled δ-NbC_{min} to the respective minimum concentration of carbon given in Table I. The parameter a describes the dependence of diffusivity on the concentration of carbon (Fig. 6).

Table IV. Diffusion Coefficients of Nitrogen in Niobium and Niobium Nitrides*

	D from the Profile Fitting			D from the Layer Growth (FFD)		
T (°C)	δ-NbN_{max} (cm²/s)	δ-NbN_{min} (cm²/s)	a (cm³/mol)	δ-NbN_{1-x} (cm²/s)	β-Nb_2N (cm²/s)	α-Nb(N) (cm²/s)
1400	$1.6(1) \times 10^{-10}$	$2.6(2) \times 10^{-10}$	21	$2.26(5) \times 10^{-10}$	$6.2(4) \times 10^{-11}$	$8.0(1) \times 10^{-9}$
1500	$6.7(3) \times 10^{-10}$	$9.1(4) \times 10^{-10}$	17	$8.30(5) \times 10^{-10}$	$3.8(3) \times 10^{-10}$	$2.0(1) \times 10^{-8}$
1600	$1.8(1) \times 10^{-9}$	$2.4(2) \times 10^{-9}$	16	$2.70(5) \times 10^{-9}$	$1.6(1) \times 10^{-9}$	$5.0(1) \times 10^{-8}$
1700	$4.5(4) \times 10^{-9}$	$6.7(5) \times 10^{-9}$	21	$7.20(5) \times 10^{-9}$	$5.5(3) \times 10^{-9}$	$1.1(1) \times 10^{-7}$
1800	$1.3(1) \times 10^{-8}$	$2.1(2) \times 10^{-8}$	23	$1.95(5) \times 10^{-8}$	$1.4(1) \times 10^{-8}$	$2.0(1) \times 10^{-7}$

*The diffusion coefficients listed in the column labeled δ-NbN_{max} correspond to the maximum nitrogen concentration, and the diffusion coefficients listed in the column labeled δ-NbN_{min} to the respective minimum concentration of nitrogen given in Table II. The parameter a describes the dependence of diffusivity on the concentration of nitrogen (Fig. 6).

tion [8] was derived from the first Fick's law,

$$J = -D \frac{\partial c}{\partial x} \qquad [9]$$

by approximating the concentrations in three adjacent points by a parabolic function.

III. EXPERIMENTAL

Reaction diffusion samples were prepared in the form of wedges, as described previously.[3,4] Such a sample shape is advantageous for the investigation of layer growth enhancement and for the calculation of diffusion coefficients in all phases from a single microstructure.[6,14] The homogeneity ranges of carbon and nitrogen in the individual phases, which were used for calculation of the nonmetal diffusion coefficients from the layer growth, are listed in Tables I and II. The measured concentrations were recalculated to mol/cm³ to take into account the crystal lattice expansion (the volume changes) occurring during the diffusion process. As niobium nitride has a high nitrogen equilibrium pressure, increasing nitrogen pressures were established with increasing temperatures to keep the surface concentration constant (Table II). Only the surface concentration measured in the sample annealed at 1400 °C differed from this value. The pressure was set to 30 bar N_2 to examine the influence of the homogeneity range width on the concentration dependence of the nitrogen diffusion coefficient in δ-NbN (refer to Section V). With our experimental facility, the surface nitrogen concentration of [N]/[Nb] = 1 could not be reached at other temperatures because of the high nitrogen pressure.

IV. RESULTS

Concentration profiles were measured using wavelength-dispersive electron probe microanalysis (EPMA). Details on the measurement are described elsewhere.[16] As the precision of EPMA decreases with decreasing concentration of light elements in the host structure, only the concentration profiles measured in the δ phases are usually considered for calculation of concentration-dependent dif-

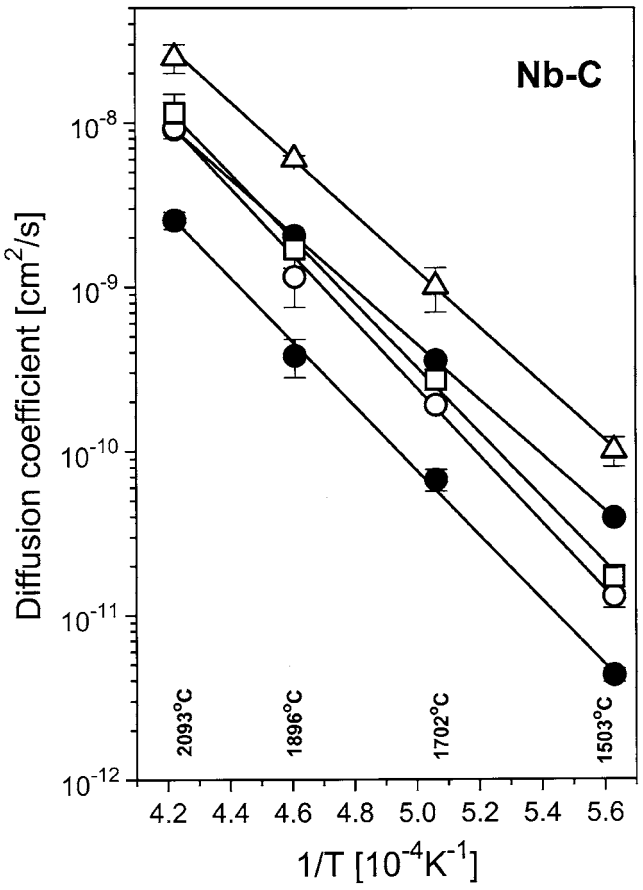

Fig. 2—Diffusion coefficients of carbon in niobium and niobium carbides at one glance. The maximum and the minimum concentration-dependent diffusion coefficients of carbon in δ-NbC_{1-x} obtained from profile fitting are plotted by solid circles. Concentration-independent diffusion coefficients calculated using the FFD method are plotted by open symbols: by triangles for α-Nb(C), by squares for β-Nb_2C, and by circles for δ-NbC_{1-x}.

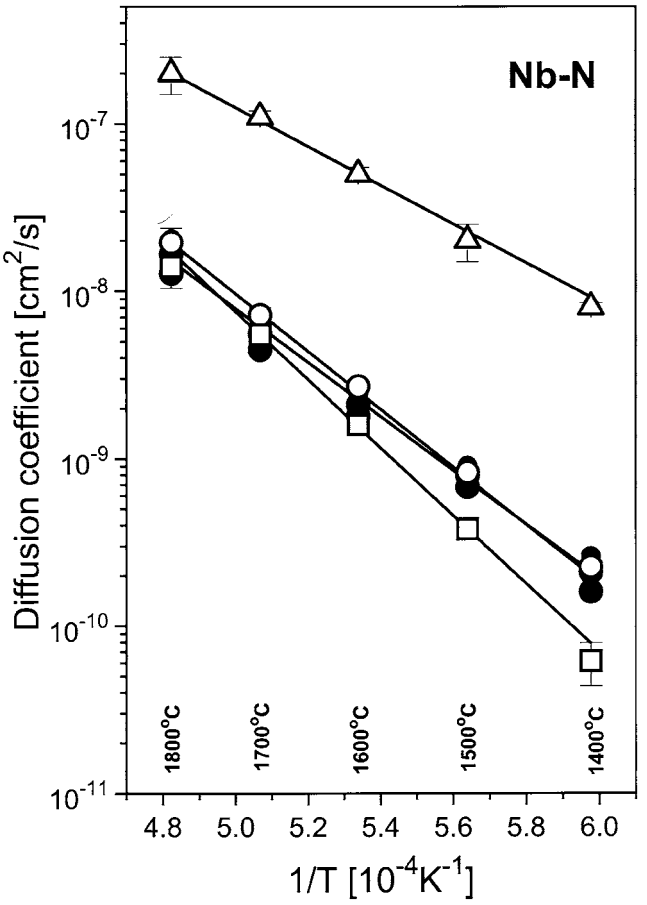

Fig. 3—Diffusion coefficients of nitrogen in niobium and niobium nitrides. Symbol assignment: the concentration-dependent diffusion coefficients of nitrogen in δ-NbN_{1-x} obtained from profile fitting are plotted by solid circles; and the concentration-independent diffusion coefficients calculated using the FFD method are plotted by open symbols. Triangles are for α-Nb(N), squares for β-Nb_2N, and circles for δ-NbN_{1-x}.

fusion coefficients. Although the concentration profiles were very smooth, even in β-Nb_2C and β-Nb_2N, they were not suitable for fitting because of the narrow homogeneity ranges. Diffusion coefficients in these phases were obtained from the layer growth.

In the first approach, the diffusion coefficients obtained by fitting the concentration profiles measured by the analytical function (Eq. [3]) were applied as an input for the evaluation of diffusion coefficients based on layer growth. These data, together with the positions of the phase boundaries, were used to calculate the complete set of diffusion coefficients in wedge-shaped samples.[6] Finally, the simulation of the diffusion process using the FFD method allowed the concentration-independent diffusion coefficients to be refined and the concentration profiles in all phases to be calculated. The FFD simulation of the reactive diffusion was performed by use of the MATLAB* environment.

*MATLAB is a trademark of The Math Works, Inc., Mass., USA.

The diffusion coefficients of carbon and nitrogen in various phases, together with their dependence on concentration, are summarized in Tables III and IV. Arrhenius plots for diffusion coefficients in individual phases (Figures 2 and 3) yielded activation energies and pre-exponential factors, which are listed in Tables V and VI. Agreement between the measured and the calculated concentration profiles is illustrated in Figures 4 and 5 for Nb-C and Nb-N, respectively. Note that, for profile fitting (Figures 4(a) and 5(a)), a least-squares routine was used to arrive at the best match of the measured and the calculated concentrations, whereas with the FFD procedure the concentration profiles (Figures 4(b) and 5(b)) were calculated as a by-product. Only the positions of the phase boundaries were compared in the FFD method, not the concentration profiles.

V. DISCUSSION

The diffusivity of carbon in niobium carbides (δ-NbC_{1-x} and β-Nb_2C) and in niobium increases monotonously with a decreasing concentration of carbon (Figure 2). Also, within δ-NbC_{1-x}, the diffusion coefficient of carbon increases with a decreasing carbon concentration. The steep dependence of the diffusion coefficient in δ-NbC_{1-x} is the main reason for the observed discrepancy between the measured concentration profile and the concentration profile calculated using FFD (Figure 4(b)). A constant diffusion coefficient, assumed in the FFD calculation, could not describe the concentration profile correctly. If the concentration profile was fitted by Eq. [3] without taking the

Table V. Activation Energies and Pre-Exponential Factors Calculated from the Temperature Dependence of the Carbon Diffusivity in Niobium and Niobium Carbides

	Profile Fitting		Forward Finite Differences		
	δ-NbC (High c)	δ-NbC (Low c)	δ-NbC_{1-x}	β-Nb_2C	α-Nb(C)
E (eV)	3.86 ± 0.13	3.35 ± 0.20	3.97 ± 0.14	3.95 ± 0.10	3.40 ± 0.10
D_0 (cm^2/s)	$0.4^{+0.4}_{-0.2}$	$0.12^{+0.4}_{-0.2}$	$2.3^{+3.0}_{-1.3}$	$2.9^{+2.3}_{-1.3}$	$0.45^{+0.13}_{-0.10}$

Table VI. Activation Energies and Pre-Exponential Factors Calculated from the Temperature Dependence of the Nitrogen Diffusivity in Niobium and Niobium Nitrides

	Profile Fitting		Forward Finite Differences		
	δ-NbN (High c)	δ-NbN (Low c)	δ-NbN_{1-x}	β-Nb_2N	α-Nb(N)
E (eV)	3.19 ± 0.10	3.20 ± 0.10	3.32 ± 0.03	4.0 ± 0.1	2.44 ± 0.04
D_0 (cm^2/s)	$0.68^{+0.59}_{-0.31}$	$1.10^{+1.02}_{-0.53}$	$2.2^{+0.4}_{-0.3}$	$1.2 \times 10^2{}^{+1.7}_{-0.7}$	$1.8 \times 10^{-1}{}^{+0.6}_{-0.4}$

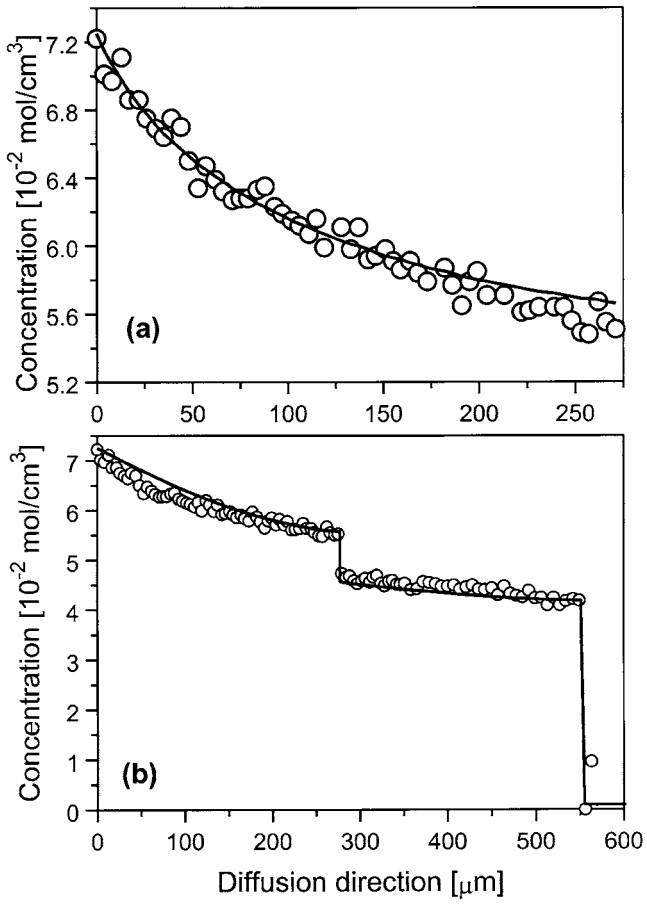

Fig. 4—(*a*) Comparison of concentration profiles measured in δ-NbC_{1-x} using EPMA/WDS (open circles) with the concentration profile calculated with diffusion coefficient depending on concentration (solid line). (*b*) Phase band structure and concentration profiles observed in the Nb-C system (open circles) and simulated using the FFD method (solid line). The sample was annealed 183 h at 1700 °C.

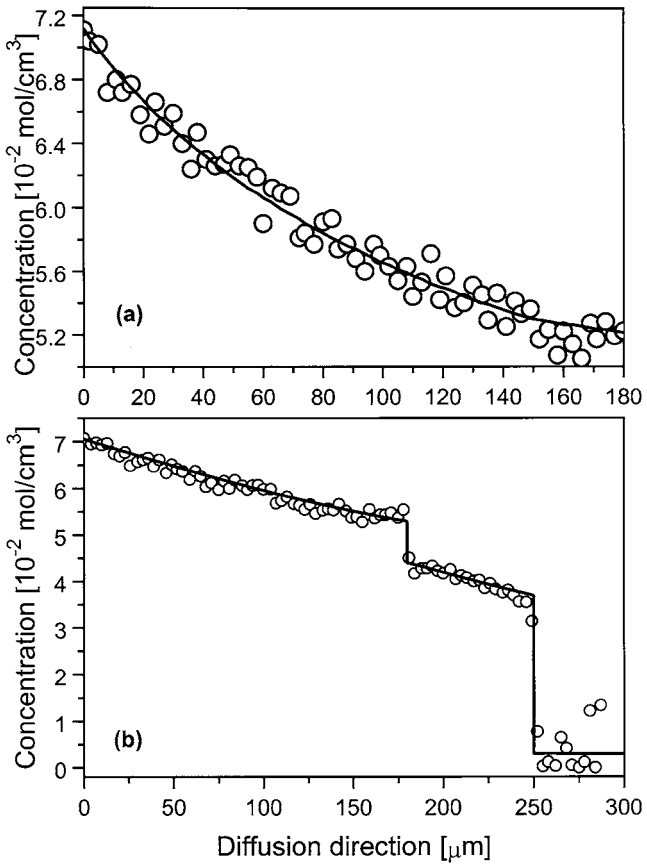

Fig. 5—(*a*) Comparison of concentration profiles measured in δ-NbN_{1-x} using EPMA/WDS (open circles) with the concentration profile calculated with diffusion coefficient depending on concentration (solid line). (*b*) Phase band structure and concentration profiles observed in the Nb-N system (open circles) and simulated using the FFD method (solid line). The sample was annealed 16 h at 1600 °C.

concentration dependence of the diffusivity in δ-NbC_{1-x} into account, the least-squares procedure yielded too-low diffusion coefficients because the calculation is controlled by the best match at individual points of a concentration profile. Furthermore, the value of the diffusion coefficient depended strongly on the weighting method used for the least-squares procedure when the concentration dependence of the diffusion coefficient was omitted. In other words, if the high concentrations measured at the sample surface were preferred, the calculated diffusivity became lower. On the other hand, if the weighting on the high concentrations

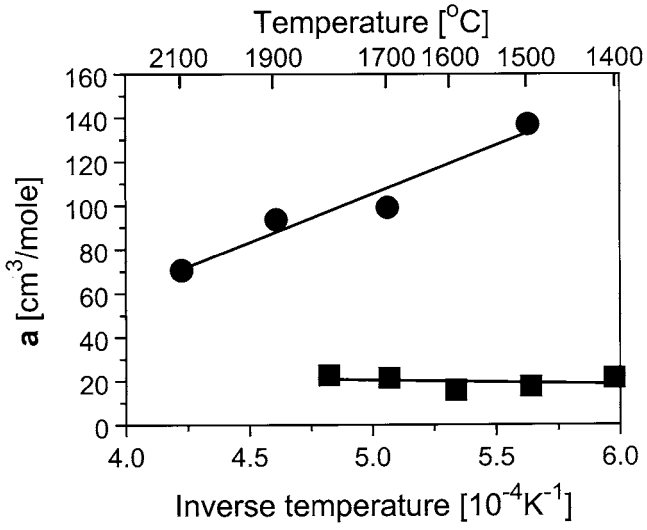

Fig. 6—Temperature dependence of the parameter a (Eq. [10]) describing the concentration dependence of the carbon and nitrogen diffusivity in δ-NbC_{1-x} (circles) and δ-NbN_{1-x} (boxes). No influence of the nitrogen pressure and the surface concentration on a was observed.

was suppressed, the calculated diffusivity became higher, as it corresponds to the dependence of the diffusion coefficient on the concentration of in-diffusing species (the higher the nonmetal content, the lower the diffusion coefficient). Conversely, the FFD method yielded concentration-independent diffusion coefficients that were correctly averaged over all concentrations, as this method works with layer growth. Diffusion coefficients obtained using FFD are between the maximum and the minimum diffusivity calculated from the concentration profiles (Figure 2). Using the diffusion coefficients obtained using the FFD method, the phase band structure can be correctly predicted by reverse calculation (several examples are given at the www server http://info.tuwien.ac.at/physmet/images.html).

The activation energy for the reactive diffusion of carbon in the Nb-C system decreases with decreasing carbon concentration, *i.e.*, the highest activation energy was observed in the carbon-rich phase δ-NbC_{1-x}, the lowest activation energy in the solid solution α-Nb(C). The changes in the activation energy are also reflected by the temperature dependence of the parameter a that describes the concentration dependence of the diffusion coefficient. In the exponential approximation of Eq. [4], the parameter a is a linear function of the reciprocal temperature (Figure 6), since it can be regarded as a coefficient describing the linear dependence of the activation energy on the nonmetal concentration.

$$D = D_0 \exp\left[-a(c - c_{\max})\right] \exp\left(-\frac{E}{k_B T}\right) = D_0 \exp\left[-\frac{E + a(c - c_{\max})\, k_B T}{k_B T}\right] \quad [10]$$

The course of diffusivity in the Nb-N system is different from that of the Nb-C system. The nitrogen diffusion coefficients do not increase monotonously with decreasing nitrogen concentration, *i.e.*, the diffusivity in the intermediate phase β-Nb_2N is smaller than or equal to the nitrogen diffusivity in δ-NbN_{1-x}. The dependence of the diffusion coefficient on the nitrogen concentration in δ-NbN_{1-x} is very weak. This was found by the concentration profile fitting and confirmed by two additional experiments done at 1700 °C, in which different nitrogen pressures (2 and 30 bar N_2) were applied. In these diffusion couples, the layer thicknesses were different (the β-Nb_2N/δ-NbN_{1-x} thickness ratio was 0.45 for 2 bar N_2 and 0.53 for 30 bar N_2, respectively), which is a consequence of the different surface concentrations, but the diffusion coefficients calculated from layer growth were the same for both samples. The weak dependence of the nitrogen diffusion coefficient on the nitrogen concentration in δ-NbN_{1-x} also resulted in a good agreement between the measured concentration profiles and the concentration profile calculated using the FFD method (Figure 5(b)).

The diffusion of nitrogen in the α-Nb(N) solid solution is characterized by the lowest activation energy. The highest activation energy was found in the intermediate phase β-Nb_2N. No significant changes in the activation energy among different nitrogen concentrations in δ-NbN_{1-x} were detected, unlike in δ-NbC_{1-x}. The different behavior of the concentration dependence of the activation energy in δ-NbN_{1-x} and δ-NbC_{1-x} could be explained by the different occupancies of metal sublattices in these two phases. In δ-NbC_{1-x}, the occupancy of the metal sites remains constant in the whole concentration range, whereas it decreases with increasing nitrogen concentration in δ-NbN_{1-x}.[17]

VI. CONCLUSIONS

The diffusion coefficients of carbon and nitrogen in niobium carbides and nitrides were calculated using a combined refinement. This method yielded two independent sets of diffusion coefficients that could be compared. One set was calculated from concentration profiles, the other from investigation of the layer growth enhancement in wedge-shaped diffusion couples. The first technique yielded the concentration-dependent diffusion coefficients in δ-NbC_{1-x} and δ-NbN_{1-x}; the second yielded the concentration-independent diffusion coefficient in all phases.

The concentration profile fitting is a suitable method for the calculation of diffusion coefficients in the nonmetal-rich phases δ-NbC_{1-x} and δ-NbN_{1-x}. In the intermediate phases, β-Nb_2C and β-Nb_2N, this method could not yield reliable diffusion coefficients because the phases exist only in a narrow homogeneity range. Consequently, just a negligible relief effect arising during the polishing of the samples can substantially influence the shape of the measured concentration profile, which makes the calculation of diffusion coefficients from the concentration profiles impossible. In the solid solutions α-Nb(C) and α-Nb(N), the concentration of the respective metalloid is too low to reach a sufficient precision and a low scatter in the measured concentrations.

On the contrary, both methods, which employed the enhanced layer growth in wedge-shaped samples to calculate the diffusion coefficients in all phases, require only the maximum and the minimum concentrations. Both can more easily be obtained than the complete concentration profiles. Consequently, it is useful to combine the diffusion coefficients obtained by fitting the concentration profiles mea-

sured by the analytical function of Eq. [3] with the diffusion coefficients obtained by investigating layer growth.

ACKNOWLEDGMENTS

One of the authors (DR) acknowledges the financial support of the ''Lise-Meitner-Post-Doctoral-Fellowship,'' No. M-00315-CHE, and of the Project No. P-8487 through the Austrian ''Fonds zur Förderung der Wissenschaftlichen Forschung.'' Calculations were performed on a SUN workstation granted by the Oesterreichische Nationalbank under Project No. 5414.

REFERENCES

1. F.J.A. den Broeder: *Scripta Metall.*, 1969, vol. 3, p. 321.
2. F.J.J. van Loo and G.F. Bastin: *Metall. Trans. A*, 1989, vol. 20A, pp. 403-11.
3. H. Wiesenberger, W. Lengauer, and P. Ettmayer: *Acta Mater.*, in press.
4. M. Joguet, W. Lengauer, M. Bohn, and J. Bauer: *J. Alloys Comp.*, in press.
5. W. Jost: *Diffusion in Solids, Liquids and Gases*, Academic Press, Inc., New York, NY, 1960, pp. 71-72.
6. D. Rafaja, W. Lengauer, and P. Ettmayer: *Acta Mater.*, 1996, vol. 44, pp. 4835-44.
7. M.A.J. Somers and E.J. Mittemeijer: *Metall. Mater. Trans. A*, 1995, vol. 26A, pp. 57-74.
8. R.E. Pawel: *J. Nucl. Mater.*, 1974, vol. 49, p. 281.
9. H.J. Christ and B. Illschner: *Scripta Metall.*, 1983, vol. 17, p. 631.
10. H. Matzke: in *The Physics and Chemistry of Carbides, Nitrides and Borides*, R. Freer, ed., Kluwer Academic Publishers, Hingham, MA, 1990.
11. R. Musenich, P. Fabbricatore, G. Gemme, R. Parodi, M. Vivani, B. Zhang, V. Buscaglia, and C. Bottino: *J. Alloys Comp.*, 1994, vol. 209, p. 319.
12. J. Crank: *The Mathematics of Diffusion*, 2nd ed., Oxford University Press, Oxford, United Kingdom, 1987.
13. F.J.J. van Loo, W. Wakelkamp, G.F. Bastin, and R. Metselaar: *Solid State Ionics*, 1989, vols. 32–33, p. 824.
14. W. Lengauer, D. Rafaja, R. Täubler, C. Kral, and P. Ettmayer: *Acta Metall. Mater.*, 1993, vol. 41, p. 3505.
15. W.F. Ames: *Numerical Methods for Partial Differential Equations*, Academic Press, New York, NY, 1977, ch. 4.
16. W. Lengauer, J. Bauer, M. Bohn, H. Wiesenberger, and P. Ettmayer: *Mikrochim. Acta*, 1997, vol. 124, p. 279.
17. W. Lengauer and P. Ettmayer: *Monatsh. Chem.*, 1986, vol. 117, p. 275.